JOURNAL OF MATERIALS SCIENCE 6 (1971) 19–24

A Study of Grain-Boundary Grooving at the Platinum/Alumina Interface

M. McLEAN, E. D. HONDROS
Division of Inorganic and Metallic Structure, National Physical Laboratory, Teddington, Middlesex

Grain-boundary grooving at the interface between solid platinum and solid alumina has been studied and its relevance to spheroidisation and particle coarsening noted. Analysis of the equilibrium shape of the grooves in conjunction with zero creep studies on platinum shows that the platinum/alumina interfacial energy is 1050 ergs/cm² at 1400° C. The rate of growth of the grooves shows that volume diffusion is the operative mass transport mechanism at all temperatures considered (1240 to 1540° C); however, there are indications that diffusion through the metal is rate-determining at lower temperatures (< 1410° C) while diffusion through the ceramic phase predominates at higher temperatures.

1. Introduction

Mass transport driven by capillary forces occurs in many phenomena in materials science (e.g. sintering [1], spheroidisation [2], particle coarsening [3].) In particular, the high temperature mechanical properties of dispersion strengthened and fibre-reinforced materials are critically altered by changes in the size and morphology of the reinforcing phases.

Analysis of the equilibrium configuration and the growth kinetics of grain-boundary grooves at free crystal surfaces have yielded valuable information concerning surface energies and capillarity-induced mass transport [4] (both by surface and volume self-diffusion). This approach has recently been applied by Feingold *et al* [5] to a solid/solid interface. The interfacial energies and mass transport parameters measured in grain-boundary grooving experiments are identical to those relevant to spheroidisation and particle-coarsening.

This paper reports results of absolute interfacial energies and mass transport parameters from grain-boundary grooving studies on the system: solid platinum bonded to solid alumina. The study on this model system was undertaken to complement work now in progress on the thermal stability of fibre- and dispersion-reinforced composite materials.

2. Relevance of Grain-boundary Grooving to Coarsening and Spheroidisation

When a dispersed phase is chemically inert with, and only sparingly soluble in, a matrix, the then mean particle radius, $\bar{r}$, of spherical particles increases with time [3]:

$$\bar{r}^n \alpha t \tag{1}$$

where $n = 2$ if transfer of material across the interface (interface control), $n = 3$ if diffusion through the matrix or $n = 4$ if diffusion along the matrix grain boundaries is the rate-determining process. For the particular case of volume-diffusion control [3]:

$$\bar{r}^3 = \frac{8}{9} Kt \tag{2}$$

where

$$K = \frac{\gamma c_0 D_V V_M^2}{RT} \tag{3}$$

γ = interfacial energy; V_M = molar volume of the dispersed phase; RT = thermal energy. The product $c_0 D_V$ has the dimensions of "concentration × solubility".

A fibre embedded in a matrix is an unstable configuration since the total surface energy may be reduced by the fibre breaking into a string of spheres. The rate of such spheroidisation, V, is related to the original radius, R_0, of the fibre [2]:

$$V \alpha \frac{1}{R_0^n} \tag{4}$$

where n has the same meaning as in equation 1. Again, when volume-diffusion controls [2]:

$$V = \frac{\alpha K}{R_0^3} \tag{5}$$

where K is as defined in equation 3 and α is a dimensionless constant.

In order to characterise the thermal stability of the strengthening phase in a composite material it is necessary to determine (i) which mass transport mechanism is operative (i.e. the value of n in equations 1 and 4), and (ii) the magnitude of the mass transport constant (i.e. of K in equations 2 and 5 if volume-diffusion controls).

Li *et al* [6] have extended Mullins, [7, 8] analysis of the growth of grain-boundary grooves to apply to multi-component systems. The dimensions of the groove (see fig. 1) as a function of time are:

$$w^n \text{ (or } d^n) \; \alpha \; t \tag{6}$$

where n has the same meaning as in equations 1 and 4. When volume-diffusion is rate-controlling

$$w^3 = 125 \; Kt \tag{7}$$

where K is again as defined in equation 3. Study of the growth of grain-boundary grooves therefore, provides a convenient measure of the parameters n and K.

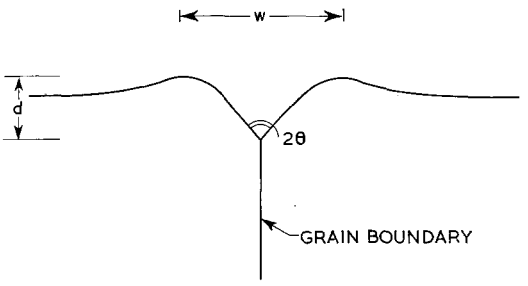

Figure 1 Schematic profile of a grain-boundary groove.

The angle subtended at the root of the groove provides a measure of the relative interfacial energies [9]. For the schematic groove shown in fig. 1:

$$\sigma = 2\gamma \cos \theta \tag{8}$$

where σ, γ are the grain-boundary and interfacial energies respectively, assumed to be isotropic. Consequently, if grain boundaries occur in both the metal and ceramic phases the relative values of all the interfacial and surface energies may be determined (see fig. 2). Then

$$\begin{aligned} \gamma_{M/M} &= 2\gamma_{M/V} \cos \theta_1 = 2\gamma_{M/C} \cos \theta_2 \\ \gamma_{C/C} &= 2\gamma_{M/C} \cos \theta_3 = 2\gamma_{C/V} \cos \theta_4 \end{aligned} \tag{9}$$

where the subscripts M, C and V indicate the interfaces between metal, ceramic and vapour. If the absolute value of any one of interfacial energies is known then the other five may be readily determined from equation 9.

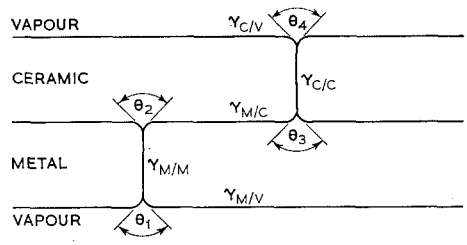

Figure 2 Schematic section of a metal/ceramic couple showing the various possible grooves.

3. Experimental Techniques

Platinum was bonded to thin plaques of α-alumina by two methods:

(i) Platinum foil was held, with various loads, in contact with the alumina at temperatures close to, but below, the melting-point of platinum: islands of good bonding were obtained by this method.

(ii) Drops of platinum were melted onto the alumina plaques in air and then cooled slowly. The platinum was sectioned parallel to, and about 1 mm from, the platinum/alumina interface. The deformation introduced in the sectioning procedure caused the platinum to recrystallise on annealing, thus producing grain boundaries normal to, and extending through, the platinum sheet. Uniform adhesion was obtained over the entire platinum/alumina interface.

The specimens were annealed in air at various temperatures in the range 1240 to 1540° C. The rate of development of the groove formed at the intersection of the platinum grain boundary with the platinum/alumina interface was monitored by interference microscopy, the interface being viewed through the transparent alumina. The maximum thickness of alumina plaques used was governed by the working distance of the objective of the interference microscope, 0.5 mm in this case. The true dihedral angle, θ, was obtained from the equation:

$$\tan \theta = \frac{2\mu L}{\lambda M} \tan \alpha \tag{10}$$

where 2α is the apparent dihedral angle measured from the interferograms; λ is the wavelength of light (corrected for aberrations), M is the lateral

magnification, L is the fringe spacing, and μ is the refractive index of alumina.

The groove-shape analysis was also performed on alumina surfaces from which the platinum had been stripped subsequent to annealing. The grooves formed at the platinum grain boundaries were replicated as ridges on the alumina surface and could be examined by conventional interference microscopy. This method, being destructive, could not be used in the study of the kinetics of groove growth.

The absolute value of the surface energy of platinum annealed in air was determined at 1400° C, using a zero-creep technique [10]. Platinum foil, 10 μm thick, was formed into a cylinder and platinum weights sintered at various points along the cylinder. The rates of extension, or contraction, of various parts of the cylinder were determined as a function of applied stress. The critical stress, σ_c, where there is effectively no movement, was determined by interpolation from the above data, and the surface energy was calculated using the expression [10]

$$\gamma = \frac{\sigma_c}{\left(\frac{1}{t} - \frac{1}{6d}\right)} \qquad (11)$$

where t is the thickness of the foil and d is the average grain diameter.

4. Results

4.1. Interfacial Energies

In fig. 3 the rate of extension of the platinum foil is plotted as a function of the applied stress for platinum in air at 1400° C. The surface energy

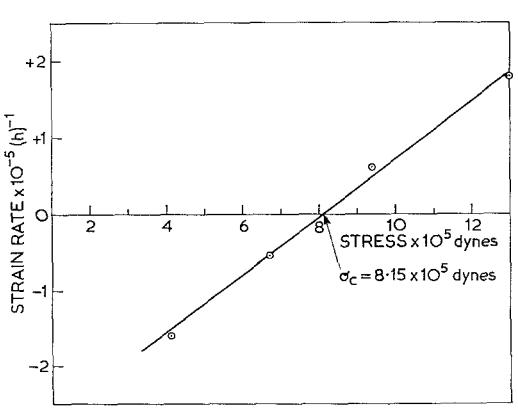

Figure 3 Strain rate of platinum foil as a function of applied stress at 1400° C.

($\gamma_{M/V}$) derived from these data, using equation 11, is 2097 ± 50 ergs cm^{-2}.

Typical interference micrographs of grooves formed at the intersection of a platinum grain-boundary with the platinum/alumina interface are shown in fig. 4. Analysis of the grooves at each extremity of the *same* grain boundaries in terms of equation 9 have yielded the relations:

$$\frac{\gamma_{M/C}}{\gamma_{M/V}} = 0.53 \pm 0.03 .$$

Similarly analysis of grooves formed by grain boundaries in alumina shows that

$$\frac{\gamma_{C/V}}{\gamma_{M/C}} = 0.68 \pm 0.10 .$$

Table I shows the absolute values of the various interfacial energies calculated from these results and all possible permutations of equation 9.

4.2. Kinetics of Groove Growth

The development of grain-boundary grooves at the platinum-alumina interface was followed as a function of time at various temperatures. Some of the interfaces faceted, indicating that the interfacial energy is anisotropic. In the following discussion we shall continue to use the isotropic form of equation 3, bearing in mind that any diffusivities derived from it may be subject to a slight systematic numerical error. This should not affect any activation energies derived from our results (see the discussion by Bonzel and Gjostein [11]).

The plots of w^3 versus t shown in fig. 5 are linear at all the temperatures considered, indicating (see equation 6) that volume-diffusion is the rate-controlling mechanism. The values of K derived from the slopes of these plots and equation 7 are listed in table II. It indicates that K is relatively insensitive to temperature below 1410° C, but increases rapidly at higher temperatures.

5. Discussion

5.1. Interfacial Energies

The surface energy of platinum in vacuum has previously been measured by a scratch decay technique, Blakely and Mykura [12]*. Combining their result with the ratio $\gamma_{air}/\gamma_{vacuum}$ determined by McLean and Mykura [13] we

*There was a numerical error in reference 12; the corrected value in vacuum is 2370 ± 750 ergs/cm^2 at 3110° C (Mykura, private communication).

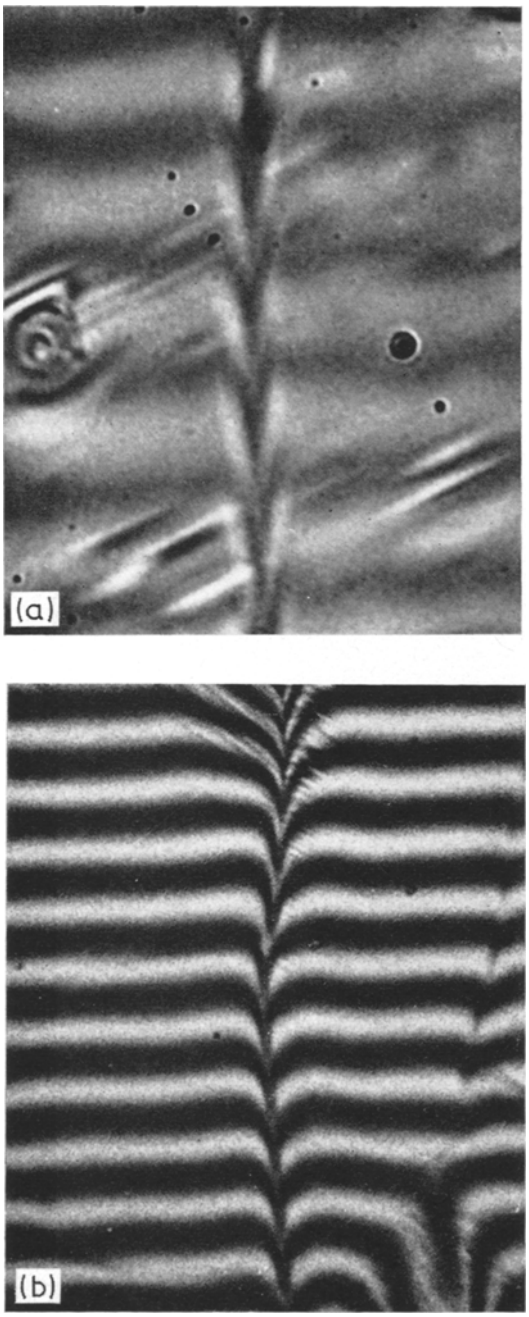

Figure 4 Interferograms of typical grooves at the platinum/alumina interface (a) viewed through the alumina and (b) replicated on the alumina surface (× 1000).

deduce that $\gamma_{M/V} = 1850 \pm 600$ ergs cm^{-2}, which is quite consistent with our result.

Furthermore, the surface energy of alumina has been determined by Kingery [14] to be 905 erg/cm^2 at 1850° C in a helium atmosphere,

TABLE I Interfacial energies in the Pt/Al_2O_3 couple at 1400° C, in air.

Interface	γ(erg cm^{-2})
Pt/air	2097 ± 50
Pt/Pt	525 ± 35
Pt/Al_2O_3	1050 ± 80
Al_2O_3/Al_2O_3	65 ± 15
Al_2O_3/air	770 ± 150

using liquid phase equilibria techniques. Our result, using an entirely different technique, of 770 ± 150 erg/cm^2 in air at 1400° C is compatible, within the error limits, with Kingery's value.

We know of no previous determination of interfacial energy of the platinum/alumina couple. However, the measured value of 1050 ± 80 erg cm^2 is considerably smaller than those found for other metal/ceramic systems [15].

5.2. Mass Transport

The rate of change of interface morphology may be controlled by (i) diffusion of one (or more) species through one of the phases, (ii) diffusion along the interface, or (iii) the transfer of one species across the interface. We have shown that mechanism (i) applies for the system under study. Moreover, since the driving forces causing coarsening and spheroidisation in composite materials are similar to those studied above, our results imply that these phenomena should also be volume-diffusion-controlled in the present experimental conditions.

The product $c_0 D_V$ has been calculated from the data of table II, the measured interfacial energy (assuming it varies negligibly with temperature) and the appropriate molar volume. It is displayed in fig. 6 as a plot of log $(c_0 D_V)$ versus $1/T$. Since the solubility is likely to be much less temperature-dependent than the diffusivity, the slope of this graph should provide a measure of the appropriate activation energy, Q, for the rate-controlling diffusion process.

TABLE II Kinetics constants for grain-boundary grooving at the Pt/Al_2O_3 interface.

Temperature (°C)	K (cm^3 sec^{-1})	$c_0 D_V$ (mole cm^{-1} sec)
1240	2.5×10^{-18}	4.3×10^{-13}
1310	3.4×10^{-18}	6.3×10^{-13}
1410	4.6×10^{-18}	9.0×10^{-13}
1510	1.8×10^{-17}	3.6×10^{-12}
1540	4.6×10^{-17}	9.6×10^{-12}

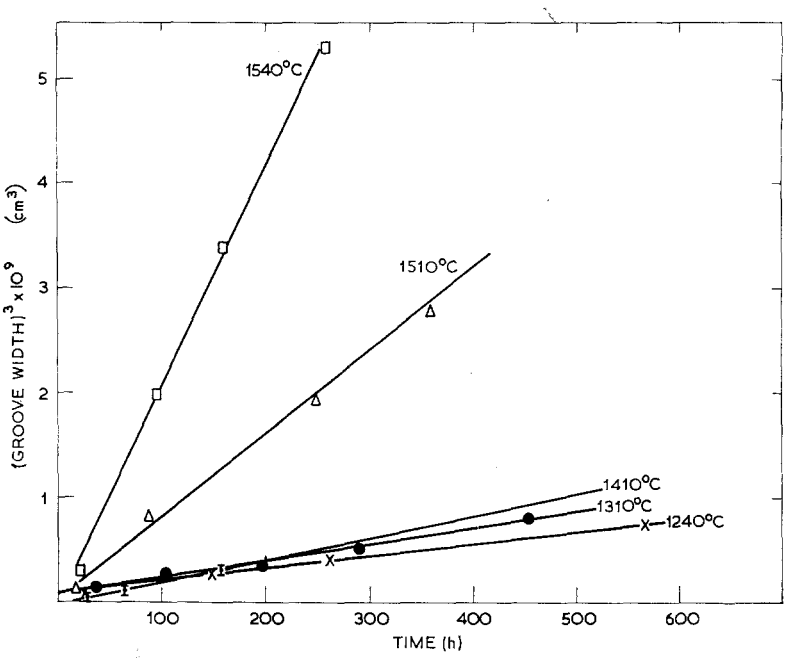

Figure 5 Plot of (groove width)^3 versus time at various temperatures.

There appear to be two temperature domains:

Domain I $T < 1410°$ C, $Q \sim 21$ Kcal/mole
Domain II $T > 1410°$ C, $Q \sim 110$ Kcal/mole

Li *et al* [6] have considered mass transport in a metal/ceramic system where the fluxes of various species are constrained to maintain their equilibrium concentrations. Qualitatively each species will diffuse by the fastest route and the slowest diffusing species will control the rate of the process. Since extrapolation of the linear portion of domain I into domain II (and vice versa) would give smaller diffusivities than those recorded, it is likely that the kink in fig. 6 is caused by the rate-controlling species diffusing in different phases in the two temperature domains.

Published data are available for self-diffusivity in platinum [16] ($Q = 67$ Kcal/mole) and alumina [17, 18] ($Q > 100$ Kcal/mole). Although diffusion of platinum in alumina has not been reported, by analogy with similar solute diffusion in Al_2O_3 the activation energy would be expected to be high (~ 100 Kcal/mole). It is likely, therefore, that in domain I diffusion of either Al or O_2 in Pt is rate-controlling. The solubility of oxygen in platinum is extremely low* ($<$ 1ppm at 1700° C). Since the product $c_0 D_V$ is important, we speculate that the diffusion of oxygen is rate-determining.

*Johnson Matthey Ltd (unpublished research).

The activation energies for the diffusion of O and Al ions in alumina are 152 and 114 Kcal/mole respectively [17, 18]. It is suggested that in domain II diffusion of either Al or O_2 in Al_2O_3 is rate-determining.

5.3. Coarsening and Spheroidisation

The analogy of grain-boundary grooving to particle-coarsening is not exact, since the latter process must involve diffusion of the particle

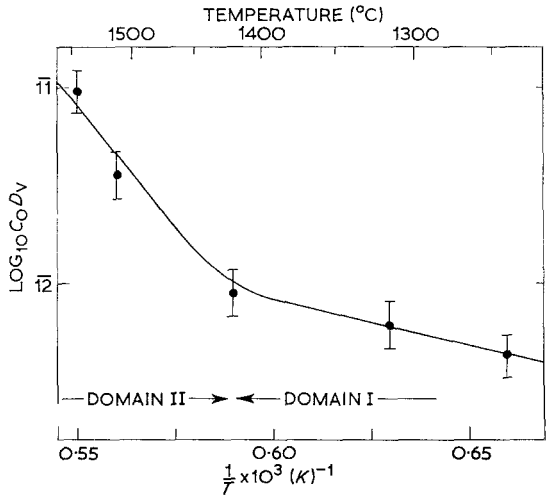

Figure 6 Plot of log ($c_0 D_V$) versus $1/T$.

phase through the matrix. Presumably the mass transport parameters relevant to coarsening of alumina dispersions in platinum at high temperatures are obtained by extrapolation of the domain I curve.

Spheroidisation of fibres may be achieved by any of the processes occurring in grain-boundary grooving, consequently fig. 6 gives the appropriate mass transport parameters.

6. Conclusions

(i) The surface energies of the platinum/air, platinum/alumina and alumina/air interfaces at 1400° C are 2097, 1050 and 770 ergs cm^{-2} respectively.

(ii) Grain-boundary grooving occurs by a volume-diffusion mechanism.

(iii) The rate-controlling mechanism is the diffusion of Al and/or O_2 through Pt below 1410° C and through Al_2O_3 above 1410° C.

Acknowledgement

This work forms part of the general research programme of the National Physical Laboratory.

References

1. F. THÜMMLER and W. THOMMA, *Metall. Reviews* no. 115 (1967).
2. F. A. NICHOLS and W. W. MULLINS, *Trans. Met. Soc. AIME* **233** (1965) 1840.
3. G. W. GREENWOOD, *Proc. Manchester Conference on* "Phase Transformations in Crystalline Solids" (*Inst. Metals, London*, 1970).
4. N. A. GJOSTEIN, in *Metal Surfaces* (*ASM, Metals* Park, Ohio, 1963).
5. A. H. FEINGOLD and CHE-YU LI, *Acta Metallurgica* **16** (1968) 1101.
6. CHE-YU LI, J. M. BLAKELY, and A. H. FEINGOLD, *ibid* **14** (1966) 1397.
7. W. W. MULLINS, *J. Appl. Phys.* **28** (1957) 33.
8. *Idem, Trans. Met. Soc. AIME* **218** (1960) 354.
9. C. S. SMITH, *ibid* **175** (1948) 15.
10. E. D. HONDROS, *Proc. Roy. Soc.* **A286** (1965) 479.
11. H. P. BONZEL and N. A. GJOSTEIN, *Phys. Stat. Sol.* **25** (1967) 209.
12. J. M. BLAKELY and H. MYKURA, *Acta Metallurgica* **10** (1962) 565.
13. M. MCLEAN and H. MYKURA, *Surface Science* **5** (1966) 466.
14. W. D. KINGERY, *J. Amer. Ceram. Soc.* **37** (1954) 42.
15. E. D. HONDROS, Chapter in Proc. of Conference on "Interfaces", Melbourne, August (1969) (Butterworth, London, 1970).
16. G. V. KIDSON and R. ROSS, "Radio-Isotopes in Scientific Research" ed. R. C. Exterman, **1** (Pergamon 1958) 185.
17. Y. OISHI and W. D. KINGERY, *J. Chem. Phys.* **33** (1960) 480.
18. A. E. PALADINO and W. D. KINGERY, *ibid* **37** (1962) 957.

Received 16 October and accepted 24 October 1970.